SSC20-WK1-08

Thermal Storage for High-Power Small Satellites

Michael G. Izenson
Creare LLC
16 Great Hollow Road, Hanover, NH 03766; 603-640-2405
mgizenson@creare.com

Darin A. Knaus
Creare LLC
16 Great Hollow Road, Hanover, NH 03766; 603-640-2355
dak@creare.com

Lucas O'Neill
Creare LLC
16 Great Hollow Road, Hanover, NH 03766; 603-640-2411
LONeill@creare.com

ABSTRACT

As the power levels and sizes of small satellites grow, new capabilities become possible along with new challenges for thermal control. Greater amounts of heat must be transported across longer distances, making it more difficult to control component temperatures using simple, passive systems. This paper describes the performance of an innovative thermal storage technology for small satellite thermal control systems. The thermal storage unit helps maintain temperature stability by efficiently incorporating a solid/liquid phase-change material (PCM).

This paper describes the results of an analysis and testing program that proved the feasibility of the PCM thermal storage concept. We formulated a simple model for a high-power small satellite in an orbital thermal environment. We found that proper selection of the PCM depends on the thermal environment, thermal control system characteristics, and characteristics of the thermal load. The model shows that a properly designed thermal storage system can dramatically reduce temperature variation.

We designed and built a sub-scale PCM thermal storage unit and measured its performance with a heat pipe under conditions that simulate operation in a small satellite thermal control system. Results of these tests demonstrate the capability of the thermal control system to reduce temperature variation during transient operation.

INTRODUCTION

Thermal storage can improve and simplify thermal control for small, high-power spacecraft. These spacecraft will have the power to support advanced capabilities such as electric propulsion and high-power imaging and communications, but their performance can be limited by the need to control component temperatures. Thermal storage can enable small spacecraft to operate at high power by reducing radiator size requirements and stabilizing component temperatures.

To use thermal storage on small satellites, the technology must meet unique and challenging design requirements. A small-satellite thermal storage unit must store a large amount of heat per unit mass, have very high thermal conductance, be extremely durable, and integrate easily with passive thermal control elements such as loop heat pipes (LHPs) and conventional heat pipes.

This paper presents results of a design study and proof-of-concept experiments that support development of a high-capacity thermal storage technology for high-power small satellites.

NEED FOR THERMAL STORAGE

Large amounts of power will be available in future small spacecraft thanks to improvements in solar panel and battery technology. High-power components will

dissipate large amounts of heat, and the component powers will be limited by the ability to radiate this heat to space at low temperature. As a result, future high-power spacecraft will need two basic thermal control elements: (1) high-performance radiators, including deployable radiators for the highest powers; and (2) thermal control systems that provide a high-conductance path for heat to flow from the spacecraft internals across the radiator surface.

Typical high-power, small satellite designs have been proposed by organizations such as Northrop Grumman,[1] Advanced Solutions Inc. (ASI),[2] and the German Aerospace Center (DLR).[3] These systems have dimensions on the order of 0.5 m, power levels in the range of 50 to 200 W, and deployable radiators for heat rejection. These spacecraft have densely packed internals with heat-generating components that cannot all be mounted on radiating surfaces or coupled to radiating surfaces with thermal straps. Future satellites are expected to operate at even higher powers (up to a kilowatt).

Thermal control systems for these small, high-power spacecraft face a fundamental challenge because heat loads and the thermal radiation environment can both vary with time. Orbital and duty-cycle variations lead to design trade-offs. The most straightforward approach is to design for the worst-case scenario (high power + least favorable radiation environment), but this approach has several drawbacks: (1) large radiators, (2) possible requirements for actively pumped heat transport systems, (3) risks of overcooling during cold parts of the orbit, along with (4) attendant requirements for active heating of temperature-sensitive components and the risk of freezing cooling circuits in the radiator. The result is that significant up-mass and complexity are added to the spacecraft, all to manage peak loads that may occur over a short duration.

Basic Concept

Thermal storage can optimize the thermal control system because proper sizing of a thermal storage module (TSM) can enable the system to be sized for average power and heat rejection conditions instead of the worst case. Figure 1 illustrates the basic concept, in which the TSM is installed between the thermal load and the spacecraft radiator. The essential feature of the TSM is a very large heat capacity—that is, the TSM can absorb a large amount of heat without a large increase in temperature. If sized properly, the TSM can accommodate temporary mismatches between heat generation and heat rejection capacity by absorbing or releasing heat while stabilizing the temperatures of the heat source and radiator.

Figure 1: Thermal Storage Concept

By stabilizing both the heat source and radiator temperature, thermal storage behaves fundamentally differently than variable-conductance heat pipes or LHPs. These variable conductance devices allow radiators to become very cold when heat loads are low or when the environment is cold. The variable conductance approach often requires use of resistance heaters to prevent the system from freezing during these situations.

Application to Small Satellites

To minimize cost and complexity, small satellites typically rely on passive thermal control devices. For higher-power systems, these systems can include heat pipes and LHPs, which have no moving parts but are capable of transporting heat across long distances. Thermal storage must work efficiently with heat pipes and LHPs to be useful for high-power, small satellites.

Figure 2 shows a schematic of an LHP along with the basic thermal storage concept. LHPs are a well-known technology for thermal control, and many excellent descriptions are available in the literature.[4,5] The LHP is a closed system containing a refrigerant that vaporizes and condenses to transfer heat. Payload components inside the satellite generate heat that is absorbed by the LHP's evaporator, where liquid refrigerant vaporizes and flows through a transport line to the system radiator. Heat loss from the radiator causes the vapor to condense, and the condensed liquid then flows back to the evaporator to complete the cycle. The pressure needed to drive refrigerant flow to the radiator and back is generated by capillary forces across the liquid/vapor interface in the wick. LHPs are particularly useful for high-power small satellites because the transport lines can cover relatively long distances and can be designed to cross flexible joints such as the interface between a satellite body and a deployable radiator.

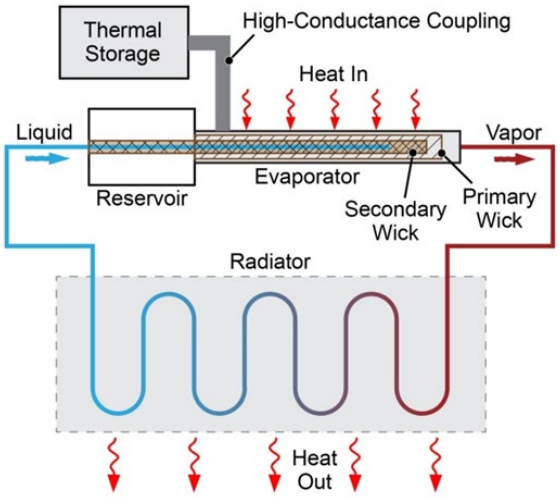

Figure 2: Implementation of Thermal Storage With a Loop Heat Pipe

Figure 2 shows thermal storage added to an LHP to improve thermal stability. By coupling to the evaporator, the TSM provides a path for heat flow in parallel with the system radiator. When heat generation exceeds the heat rejection capability of the radiator, heat will flow from the evaporator into the TSM. Likewise, when the heat flow from the radiator exceeds the rate of heat generation, heat will flow from the TSM into the evaporator. A critical requirement for temperature stability is a high-conductance coupling between the TSM and the evaporator.

PHASE-CHANGE MATERIAL FOR THERMAL STORAGE

Phase-change materials (PCMs) are ideal for thermal storage because of their capacity to absorb or liberate heat at constant temperature by melting or freezing. Paraffin wax PCM, in particular, is well suited for thermal storage on small satellites thanks to the large heat of fusion and melting points in a useful temperature range for satellite thermal control.

Basic Properties of PCM Thermal Storage

Figure 3 illustrates the property of a PCM that makes it useful for thermal storage. The figure shows schematically the relationship between heat added to a mass of PCM and the PCM temperature. At temperatures less than the melting temperature (T_{melt}), the PCM temperature increases with heat added at a rate that is proportional to the mass of PCM (m_{PCM}) and the specific heat of the solid PCM. At temperatures greater than T_{melt}, the temperature increases in proportion to m_{PCM} and the specific heat of the liquid. However, if the PCM temperature is equal to T_{melt}, then it will absorb heat without changing temperature as the solid melts. The amount of heat that can be absorbed is equal to the product of m_{PCM} and the material's heat of fusion (Δh_{sf}). The process is completely reversible, so that the PCM will liberate heat at constant temperature as the liquid freezes.

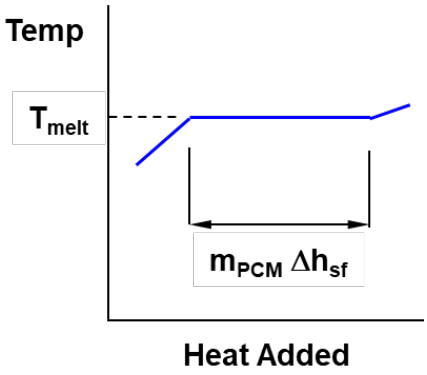

Figure 3: PCMs Absorb Heat by Melting or Freezing Instead of Changing Temperature

Paraffin Wax for Thermal Storage on Small Satellites

Paraffins (or alkanes) are simple hydrocarbon molecules with properties that are very useful for satellite thermal control. Paraffins are straight-chain, saturated hydrocarbons that are nontoxic and noncorrosive (Figure 4). At STP they are nonvolatile white solids and/or clear liquids with densities of approximately 0.8 g/cm^3.

Figure 4: Paraffin Wax is an Attractive PCM for Small Satellites[6]

Table 1 lists properties of three typical paraffins that span a range of melting temperatures that are useful for satellite thermal control. The heat of fusion (200 to 240 J/g) and density (ρ, 0.77 to 0.79 g/cm^3) do not vary much between the different paraffins. However, the melting temperature increases significantly with the molecular weight. This property allows designers to select a PCM for thermal storage that matches the

temperature requirements of a thermal control system by selecting the appropriate variety of paraffin.

Table 1: Properties of Example Paraffins[7]

	T_{melt} (°C)	Δh_{sf} (J/g)	ρ (g/cm^3)
Pentadecane ($C_{15}H_{32}$)	10	206	0.768
Octadecane ($C_{18}H_{38}$)	28	240	0.777
Icosane ($C_{20}H_{42}$)	36	241	0.789

MODEL FOR SATELLITE THERMAL ENVIRONMENT

To understand the basic thermal storage requirements for small satellites, we formulated a model that simulates the thermal environment for a small satellite in low-Earth orbit (LEO). The model allows generalized calculations of satellite thermal response that are useful for basic sizing of the TSM.

Model Basis

Figure 5 shows the basis for the LEO thermal environment model. The model is based on analysis methods published by Rickman (2014),[8] and includes simplifying assumptions that make it suitable for first-order sizing and trade-off studies. The model calculates radiation fluxes on each of the six faces of an orbiting, stabilized, box-shaped satellite due to direct solar, reflected solar (albedo), and planetary infrared radiation. The model assumes a low circular orbit and computes the radiation fluxes based on altitude, angle-to-solar vector (β), and orbital angle (θ). For LEO calculations, we assume a constant planetary surface reflectivity of 0.31. Although not discussed here, we have also adapted the model for the case of a non-stabilized satellite and used surface temperature data from Mastropietro et al. (2005)[9] to calculate the thermal environment in low-Lunar orbit.

Figure 6 shows the different phases of an orbit that determine the thermal boundary conditions, and Table 2 shows the radiation sources that are active during each orbital phase. The model comprises geometrical calculations for the magnitude of each radiation flux on each satellite face at each point in the orbit. Direct sunlight and albedo radiation have relatively short wavelengths, while the planetary IR radiation comes from a much lower temperature source and has a much longer wavelength. The distinction is important because radiator coatings typically have absorptive characteristics that differ between short and long wavelength radiation.

Table 3 lists baseline orbital parameters that we used for the illustrative calculations in this paper, and Figure 7 shows typical results from the environmental model. The figure plots the total incident radiation (in W) for a 0.5 m cubical satellite orbiting Earth at an altitude of 408 km and a β angle of 30°. We modeled radiators as surfaces perpendicular to the satellite "north" and "south" vectors (faces 5 and 6) and used typical end-of-life values for short wavelength absorptivity ($\alpha = 0.10$) and long-wavelength emissivity ($\varepsilon = 0.78$) (Gilmore 2002).[10]

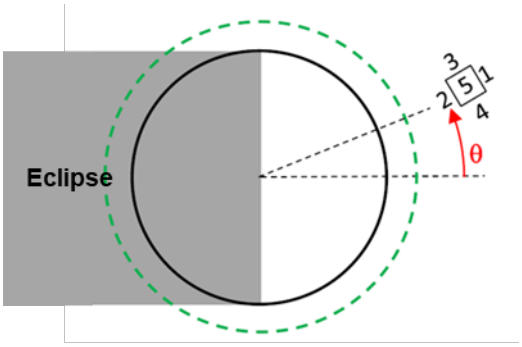

View from perpendicular to orbit plane.
Side 6 not shown

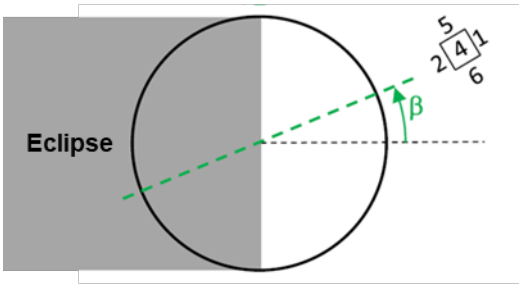

View from edge on to orbit plane.
Side 3 not shown

Figure 5: Satellite Configuration Relative to Orbital Parameters (Rickman 2014)

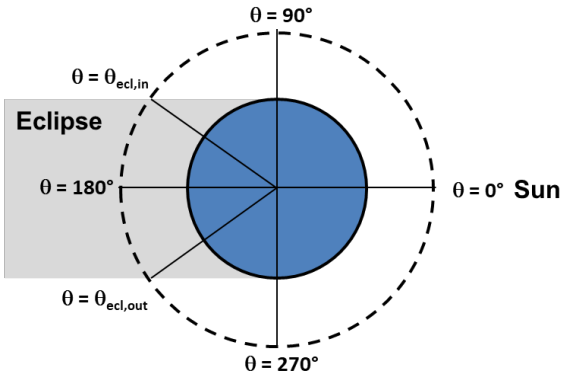

Figure 6: Orbital Phases

Table 2: Thermal Radiation Sources on Orbit

Orbital Angle, θ	Direct Sunlight	Albedo	Planetary IR
0° –90°	✓	✓	✓
90° – $\theta_{ecl,in}$	✓		✓
$\theta_{ecl,in}$ – $\theta_{ecl,out}$			✓
$\theta_{ecl,out}$ – 270°	✓		✓
270° – 360°	✓	✓	✓

Table 3: Baseline Orbital and Satellite Parameters

Altitude of circular orbit	(km)	408
Period of circular orbit	(min)	92.7
Angle between sun and orbit vectors	(°)	60
Planetary reflectivity	(-)	0.31
Absorptivity for short-wave radiation	(-)	0.10
Emissivity for long-wave radiation	(-)	0.78
Amplitude of heat generation function	(W)	400
Radiator length	(m)	0.5
Radiator width	(m)	0.5
Orbit angle at entry to eclipse	(°)	133.1
Orbit angle at exit from eclipse	(°)	226.9
Satellite dimension 1	(m)	0.50
Satellite dimension 2	(m)	0.50
Satellite dimension 3	(m)	0.50

Figure 7 shows the total incident radiation calculated for a small satellite using the parameters from Table 3. The behavior shown is the sum of the three radiation sources based on their dependence on orbital angle. Planetary albedo is constant throughout the orbit at about 110 W and is the only environmental radiation source during the eclipse period (θ = 133 to 227°). The albedo heat flux is present only on the sun-side of Earth (θ = 0 to 90° and 270 to 360°) and decreases from a maximum level at 0° to minimum levels at 90°C and 270°. The direct solar flux is active at all angles outside eclipse and has a complex dependence on orbital angle that depends on the area of the satellite that is exposed to direct sunlight. The result is a complex function of angle that varies between roughly 600 to 750 W outside of eclipse and falls to 110 W during eclipse.

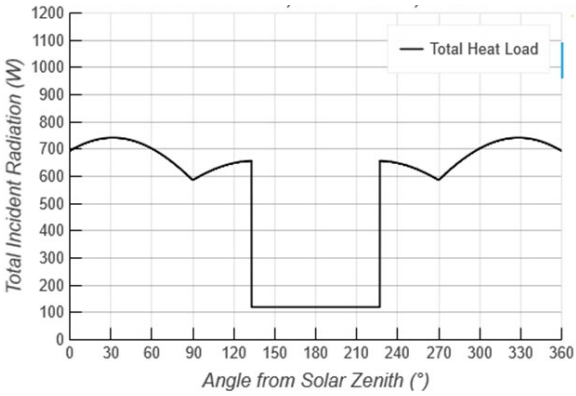

Figure 7: Total Incident Radiation for Typical LEO Parameters

MODEL FOR SATELLITE THERMAL RESPONSE

To show the benefits of PCM thermal storage for small satellites, we formulated a model for the satellite thermal control system based on a basic, two-node system architecture, conservation of energy, and a simplified model for the PCM thermal storage unit.

Thermal Control System Architecture

The orbital radiation environment provides boundary conditions for calculating the thermal behavior of an orbiting spacecraft. For general design studies of PCM thermal storage, we formulated a simplified model for the satellite thermal control system. Figure 8 is a schematic of the model illustrating the key elements:

- A heat source, modeled as a payload mass and time-dependent heat generation q(t).
- A PCM TSM that is coupled thermally to the heat source.
- An LHP that couples the heat source and TSM to the radiator.
- A satellite enclosure that insulates the heat source and TSM from direct exposure to sunlight.
- A radiator that is exposed to the external radiation environment.

The model assumes that the LHP has constant thermal conductance (W/°C) when operating in the forward direction ($T_{source} > T_{rad}$), but has zero conductance when operating in reverse. The radiator is assumed to extend from the satellite parallel to faces 5 and 6 (to minimize the incident flux of direct solar radiation), and is provided with a thermal coating with a high reflectance for short-wavelength radiation and high emittance for long-wavelength radiation.

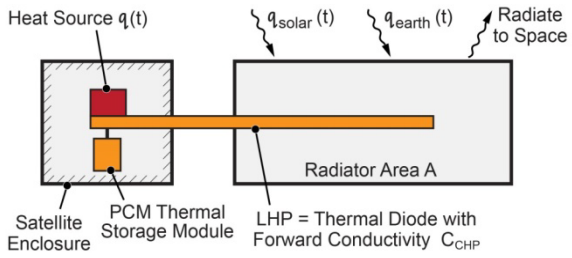

Figure 8: Simplified Model for Satellite Thermal Performance

Conservation of Energy

The thermal model is based on conservation of energy applied to the heat source and the radiator. We treat both elements as lumped thermal masses that can be characterized by single temperatures (T_{source} and T_{rad}). The heat source gains energy due to heat generated by the payload and loses energy in proportion to the difference in temperature between payload and radiator. The temperature changes at a rate that is inversely proportional to the total thermal mass of the heat source itself and the PCM TSM:

$$\dot{T}_{source} = \frac{q_{source} - C_{LHP}(T_{source} - T_{rad})}{m_{source}c_{p,source} + m_{PCM}c_{p,PCM}} \quad (1)$$

For this calculation, the specific heat of the PCM is modified to account for the heat of fusion, as described in the next section.

The radiator gains energy due to heat transfer from the payload and thermal radiation from the environment. The radiator loses energy by thermal radiation to the environment, and the rate of change of the radiator's temperature is inversely proportional to the radiator's thermal mass:

$$\dot{T}_{rad} = \frac{C_{LHP}(T_{source} - T_{rad}) + q_{rad,in} - \sigma\varepsilon A_{rad}\, T_{rad}^4}{m_{rad}c_{p,rad}} \quad (2)$$

The radiation heat input to the radiator is calculated from results of the environment calculation as follows:

$$q_{rad,in} = \sum_i \left[\alpha\, A_i \left(\varphi_{sol,i} + \varphi_{alb,i}\right) + \varepsilon\, A_i\, \varphi_{pla,i}\right] \quad (3)$$

where the subscript "i" represents each radiator face. The heat source is time-dependent, as are the values of the radiation fluxes.

The variables in equations (1) through (3) signify:

T_{source} = payload temperature (K)
m_{source} = payload mass (kg)
$c_{p,source}$ = payload specific heat (J/kg-°C)
m_{PCM} = PCM mass (kg)
$c_{p,PCM}(T)$ = PCM specific heat (models heat of fusion) (J/kg-°C)
T_{rad} = radiator temperature (K)
m_{rad} = radiator mass (kg)
$c_{p,rad}$ = radiator specific heat (J/kg-°C)
$q_{source}(t)$ = payload heat generation (W)
C_{LHP} = thermal conductance of LHP (W/°C)
$q_{rad,in}$ = heat input to radiator from environment (W)
σ = Stefan-Boltzmann constant (5.67×10^{-8} W/m^2-K^4)
ε = thermal emissivity of radiator surface for long-wavelength radiation (-)
α = the thermal absorptivity of the radiator surface for short-wavelength radiation (-)
A_{rad} = total radiation area (m^2)
A_i = area of radiator face "i" (m^2)
$\varphi_{sol,i}$ = direct solar flux on radiator face "i" (W/m^2)
$\varphi_{alb,i}$ = albedo flux on radiator face "i" (W/m^2)
$\varphi_{pla,i}$ = planetary IR flux on radiator face "i" (W/m^2)

PCM Thermal Storage

The freezing and melting behavior of the PCM is modeled using a temperature-dependent function for the specific heat that has a very large value near the melting point. Figure 9 shows the approach. For temperatures that are more than 0.5°C removed from T_{melt}, the model uses the actual values of the liquid or solid specific heats ($c_{p,liq}$, $c_{p,solid}$). For temperatures that are within 0.5°C ot T_{melt}, the model uses a value for the specific heat that is numerically equal to the heat of fusion plus the average of the liquid and solid specific heats. We choose this particular value so that energy is conserved as the PCM temperature changes across this range. Adding the average liquid/solid specific heat to the effective c_p value ensures energy conservation by accounting not only for the heat of fusion but also for the sensible heat absorption between T_{melt}-0.5°C and T_{melt}+0.5°C:

$$\int_{T_{melt}-0.5°C}^{T_{melt}+0.5°C} c_{p,PCM}(T)\, dT$$

$$= h_{PCM}(T_{melt} + 0.5°C) - h_{PCM}(T_{melt} - 0.5°C) \quad (4)$$

where $c_{p,PCM}(T)$ represents the effective specific heat and $h_{PCM}(T)$ is the actual enthalpy of the PCM.

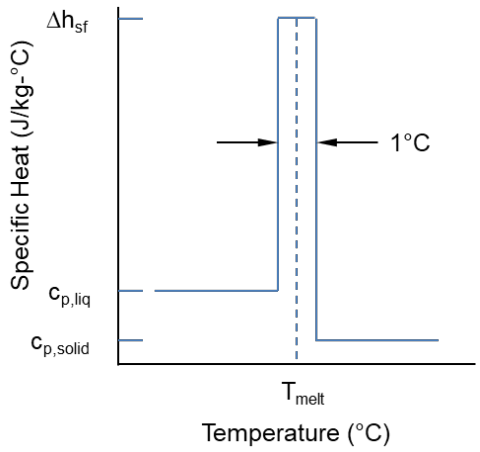

Figure 9: Model for Energy Absorption by PCM

CALCULATIONS OF THERMAL STORAGE EFFECTS

We used the combined environmental and satellite thermal models to quantify the benefits of PCM thermal storage. We found that relatively small amounts of PCM could have large benefits for temperature stability. For the most demanding applications where highly stable temperatures are needed, the choice of PCM can have a large effect on system performance.

Baseline Assumptions

We calculated the payload temperature for a small satellite based on:

- Orbital and satellite parameters listed in Table 3.
- A heat source modeled as 1 kg of aluminum.
- Payload power of 400 W with a 25% duty cycle (the power was on once per orbit during the period of maximum solar heating).
- A two-sided spacecraft radiator, parallel to faces "5" and "6" (Figure 5), with an area of 0.25 m² and made from 2 mm thick aluminum.

We varied the mass and PCM material used in the TSM depending on the case being analyzed.

Simulation Results for Pentadecane TSM

Figure 10 shows results of a series of calculations for the spacecraft thermal performance. The plots show calculated payload temperature (top) and heat sources (bottom) as a function of time for 12 orbits, which is enough time for the system to reach a nearly steady state. The bottom plot shows the heat sources used in the calculation: "rad heating" corresponds to the radiation heat input to the radiator ($q_{rad,in}$ in Eq. (2)) and "sat heat gen" is the heat generated by the satellite payload. Payload temperatures are computed for four different cases: no TSM, and TSMs comprising 0.3, 1.0, and 3.0 kg of pentadecane PCM.

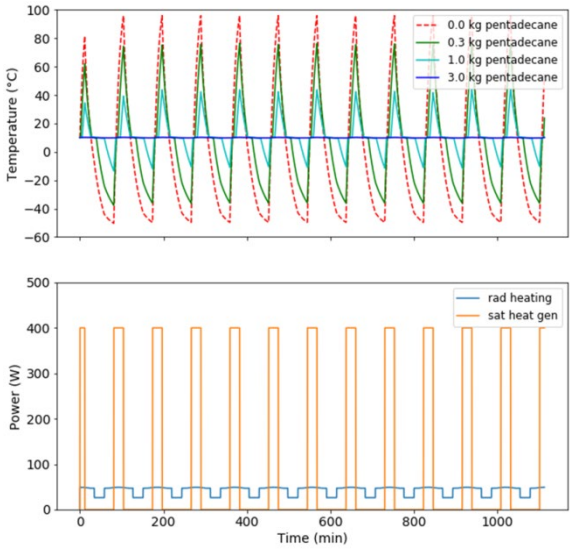

Figure 10: Heat Source Temperatures for Time-Varying Power Generation and Thermal Environment

The temperature calculations show the dramatic effects that PCM thermal storage can have on the payload temperature. Without any additional thermal storage, the payload swings between roughly +100°C and -50°C every orbit. As thermal storage is added to the system, the peak high and low temperatures converge rapidly, until with 3.0 kg of PCM the payload remains at a constant temperature throughout the entire orbital cycle.

Figure 11 plots the temperature swing (maximum – minimum temperature) as a function of pentadecane mass. Small amounts of PCM decrease the temperature swing in a very linear fashion, reducing the variation from 150°C to 60°C with 1 kg of PCM. Thermal response in this range is characterized by complete melting and freezing of the PCM as the payload passes through the melting point during each warming or cooling period, followed by temperature variation above and below the melting point. Larger amounts of PCM reduce the temperature swing further, reaching zero at about 3 kg pentadecane. At this point, the entire mismatch between heat generation and heat rejection capacity is accommodated by melting and freezing the PCM.

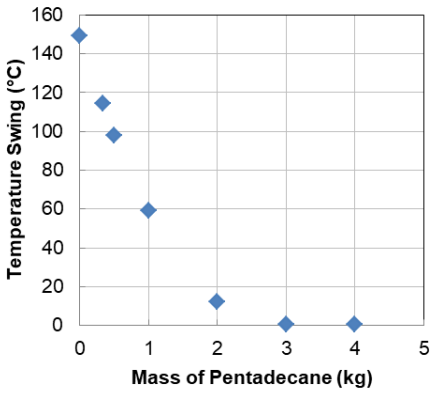

Figure 11: A Small Amount of PCM can Dramatically Reduce Orbital Temperature Variation

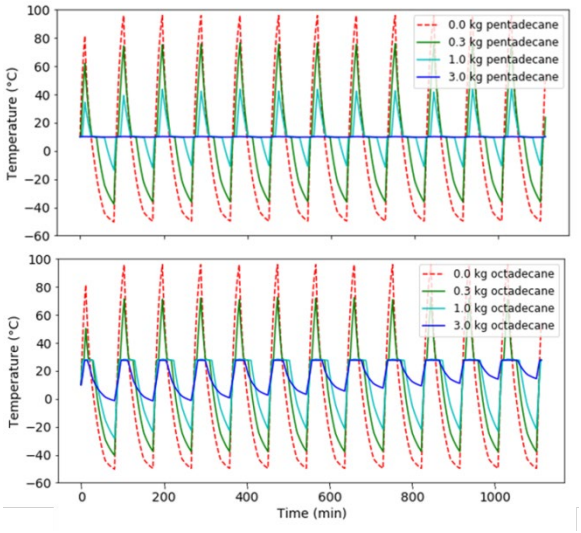

Figure 12: Choice of PCM can Have a Large Effect on Orbital Temperature Variation

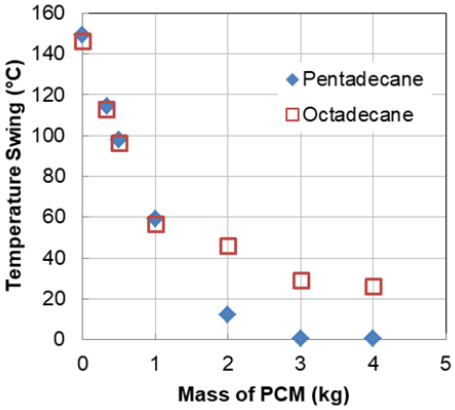

Figure 13: Calculated Orbital Temperature Swings for Pentadecane and Octadecane PCM

Choice of PCM

Changing the PCM can have significant effects on temperature stability. Figure 12 compares calculated payload temperatures for pentadecane (top plot, same as in Figure 10) and octadecane. Octadecane and pentadecane have very similar heats of fusion (Table 1), but octadecane has a higher melting point (28°C vs 10°C). The calculations show that the payload temperatures are very similar for smaller masses of PCM. However, the higher melting point of octadecane is not close to the average orbital temperature. As a result, the temperature variation with higher masses of PCM is quite different between octadecane and pentadecane. The higher melting point of octadecane means that more heat is radiated while the PCM is refreezing, which means that (1) during a temperature downswing, the entire PCM mass will freeze more quickly and then start dropping in temperature; and (2) a greater portion of the orbit will be spent with the PCM completely frozen. Figure 13 compares the temperature swings for pentadecane and octadecane as a function of PCM mass. These calculations show that care must be taken when selecting a PCM for applications that require extremely uniform temperature.

THERMAL STORAGE DEMONSTRATION

To demonstrate thermal storage, we built a proof-of-concept TSM and coupled it to a thermosiphon using prototypical high-conductance thermal link. Results show that it is feasible to use PCM to stabilize temperatures in a passive thermal control system.

Figure 14 shows the basic test concept. To simulate a passive thermal control system, we used a thermosiphon to simulate a heat pipe that transports heat from the satellite's payload to the radiator. A thermosiphon is a vertical heat pipe that uses gravity to return condensate to the evaporator instead of capillary forces. Heat is added to liquid refrigerant at the bottom of the thermosiphon, which produces vapor that condenses at the top. Heat is removed via a cooling coil at the top of the thermosiphon, and the internal saturation condition is controlled by adjusting the

temperature of the chiller. The proof-of-concept TSM was thermally linked to the thermosiphon near the condenser using a prototypical high-conductivity thermal coupling.

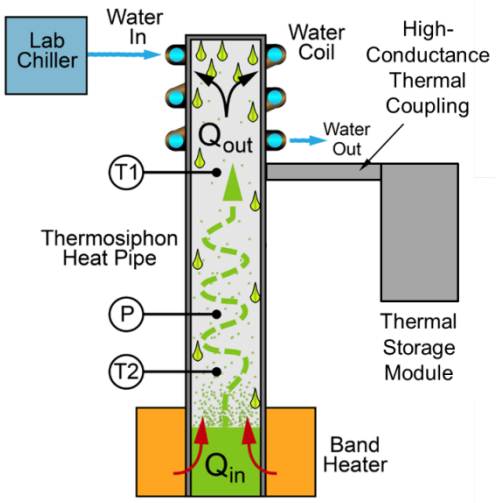

Figure 14: Proof-of-Concept Test

We built the thermosiphon from a 1 in. copper tube (Figure 15). Heat for evaporation was provided by film heaters wrapped around the bottom 5 in. of the tube, and heat was removed by cooling water flowing through a copper tube wrapped around the upper 12 in. of the thermosiphon tube. The thermal storage module was built using octadecane PCM. Key measurements during testing were the internal pressure (and corresponding saturation temperature), a condenser temperature measured by a thermocouple in the vapor space inside the thermosiphon, PCM temperatures measured by internal thermocouples, multiple surface temperatures, and the flow rate and temperature rise of condenser cooling water.

To demonstrate thermal storage, we measured the performance of the rig during power transients and compared results with and without the TSM. Figure 16 shows results of a 150 to 80 W power decrease using isopropyl alcohol as the working fluid. Without thermal storage, the system saturation temperature (black trace, Figure 16a) dropped smoothly to a new steady state condition where heat removal from the condenser balanced the new evaporator heat load. With thermal storage (red trace), the system saturation temperature held at 26°C for over five minutes as the PCM refroze and added additional heat to the rest of the system. This temperature is less than octadecane's melting temperature due to the finite thermal conductance of the proof-of-concept setup.

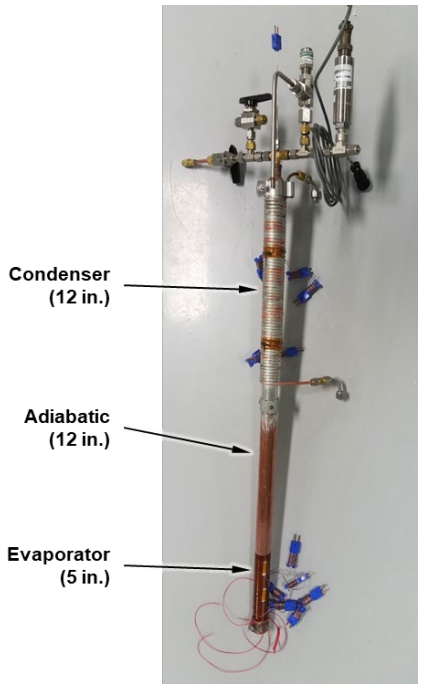

Figure 15: Thermosiphon Used for Proof-of-Concept Tests

Figure 17 shows the temperature difference measured between the inlet and exit of the condenser cooling water coil. With thermal storage, the heat rejection remained high for five minutes due to the additional heat from the freezing PCM as the temperature fell past the freezing point. The difference in condenser heat removal amounts to 15.8 kJ when integrated across the transient, which is in rough agreement with the theoretical phase change energy of the octadecane in the TSM (10.4 kJ).

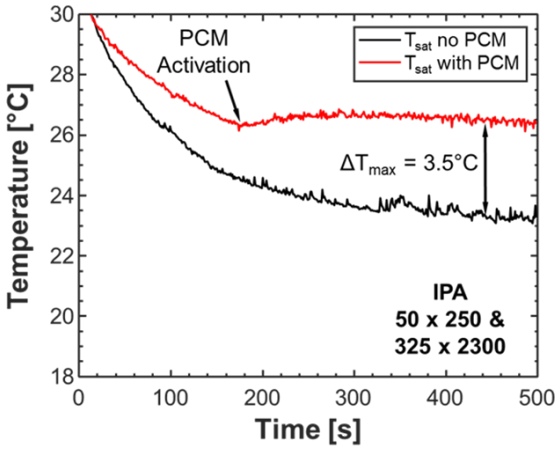

Figure 16: Demonstrated Temperature Stabilization by Thermal Coupling to PCM

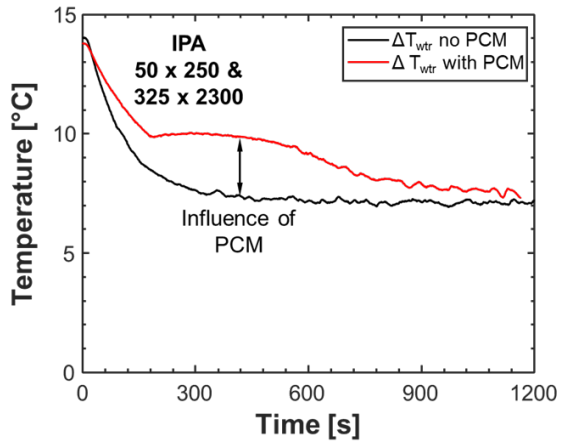

Figure 17: Calorimetry Shows Extra Heat Added by Freezing PCM

DISCUSSION

The analysis and proof-of-concept experiments illustrate the effects of PCM thermal storage on thermal control and show that highly stable temperatures can be maintained for components in small satellites.

PCM thermal storage can be used to maintain very stable temperatures for temperature-sensitive components such as batteries. The amount of PCM needed is relatively modest. In the cases analyzed in this paper, temperatures were completely stabilized using roughly 1 kg of PCM for every 140 kJ of energy dissipation per orbit.

Temperatures of components with less stringent requirements can be controlled with even smaller masses of PCM. In operating regimes where the PCM completely freezes and thaws during each orbital period, we found that the reduction in temperature variation is proportional to PCM mass and inversely proportional to the payload energy per orbit. If we define a figure of merit (FOM) as follows:

$$\Delta T_{swing} = FOM \ \frac{m_{PCM}\,\Delta h_{fs}}{E_{orbit}} \qquad (5)$$

where ΔT_{swing} is the reduction in magnitude of the heat source's cyclic temperature swing relative to no thermal storage and E_{orbit} is the energy generated by the heat source in a single orbital period. For pentadecane and the small satellite considered in the example calculations, FOM = 244°C.

Analysis shows the importance of matching the PCM material to the orbital environment and satellite thermal characteristics. Temperature variation is minimized during an orbital cycle when the melting temperature of the PCM is selected so that the sensible heat accumulation in the PCM when its temperature is above T_{melt} is roughly equal to the sensible heat loss from the PCM when its temperature is below T_{melt}.

The analysis and modeling tools described in this paper will be useful for initial system architecture and trade-off studies. More detailed modeling will be needed to solve specific, detailed satellite design problems.

The details of our TSM and high-conductivity coupling are proprietary; however, the test results described in this paper along with detailed design calculations show possibility of achieving PCM mass fractions of 46.7% and energy storage densities of 95 kJ/kg. These parameters should enable high-power small satellites to incorporate large amounts of PCM thermal storage with relatively small mass penalties.

CONCLUSIONS

We have found that major improvements in temperature stability are possible by adding small amounts of PCM thermal storage to passive thermal control systems on high-power small satellites. Based on the illustrative calculations described here, roughly 1 kg of paraffin PCM is needed per 100 W of peak power.

This assessment is based on combining results from two analysis and design models: (1) a simple model for the orbital thermal environment applicable to satellites in near circular, LEOs; and (2) a simple model for a satellite thermal control system. Measurements of TSM performance in proof-of-concept tests have shown the feasibility of using our TSM to stabilize the temperature of a high-power small satellite that is cooled by a heat pipe or LHP.

Acknowledgments

The authors gratefully acknowledge the support of the NASA Jet Propulsion Laboratory; the Propulsion, Thermal, and Materials Engineering Section; and the NASA SBIR Program.

References

1. https://rsdo.gsfc.nasa.gov/images/catalog/Eagle.pdf
2. http://www.go-asi.com/aerospace/asi-150-small-satellite-bus/
3. https://directory.eoportal.org/web/eoportal/satellite-missions/t/tet-1
4. Ku, J., "Introduction to Loop Heat Pipes," https://ntrs.nasa.gov/search.jsp?R=20150018090 2019-12-31T18:19:22+00:00Z
5. https://crtech.com/videos/part-1-overview-loop-heat-pipes

6. https://gilsonite-bitumen.com/en/products/paraffin-wax
7. https://webbook.nist.gov/chemistry/
8. Rickman, S., "Introduction to On-Orbit Thermal Environments," Presented at: 25th Annual Thermal & Fluids Analysis Workshop, 4–8 Aug 2014, Cleveland, OH.
9. Mastropietro, A., et al., "Lunar Reconnaissance Orbiter (LRO) Thermal Design Drivers and Current Thermal Design Concept," Presented at: 16th Annual Thermal & Fluids Analysis Workshop; 8–12 Aug 2005, Orlando, FL.
10. Gilmore, D. G. (ed.), Spacecraft Thermal Control Handbook, Second Edition, The Aerospace Corporation, 2002.